Thermal Contraction and Ferroelectric Phase Transition in Vinylidene Fluoride–Trifluoroethylene Copolymers. 1. An Effect of Tensile Stress along the Chain Axis

Kohji Tashiro,* Shin Nishimura, and Masamichi Kobayashi

Department of Macromolecular Science, Faculty of Science, Osaka University, Toyonaka, Osaka 560, Japan. *Received August 24, 1987*

ABSTRACT: Thermal contraction has been measured for the uniaxially oriented samples of vinylidene fluoride–trifluoroethylene (VDF–TrFE) copolymers with various VDF contents. In the heating process, for example, the bulk sample length was found to contract largely in the temperature region of the phase transition. This thermal behavior, including the dependence on VDF content, was found to intimately relate with the DSC data and the structural data such as infrared absorption and X-ray diffraction, indicating that the dimensional change in the crystalline region occurring in the ferroelectric phase transition reflects directly on the bulk dimensional change observed here. The transition point estimated from the thermal contraction curve was found to shift to the lower temperature side with an increasing tensile stress, about $-4 \sim -7$ °C/MPa. On the basis of the modified Clausius–Clapeyron equation the phenomenon was interpreted reasonably to originate from the shift in the phase-transition temperature of the crystalline region under the tensile stress. The direct measurement of the transition point shift by the X-ray diffraction under stress supported this interpretation experimentally.

Introduction

An important structural feature of the ferroelectric phase transition of vinylidene fluoride–trifluoroethylene (VDF–TrFE) copolymers is a large conformational change of the molecular chain between the extended all-trans form (below the transition temperature T_c) and the contracted gauche form (above T_c).[1-5] That is, the crystal dimension along the c axis changes largely through the phase transition. Such a dimensional change is expected to reflect directly on the macroscopic sample length. In this paper the macroscopic dimension of the uniaxially oriented samples along the draw axis was measured as a function of temperature by using a thermomechanical method under a constant tensile stress. The results are compared with those for the crystalline region, and an effect of the externally applied tensile stress on these dimensional changes will be discussed.

Experimental Section

Thermomechanical Measurements. Figure 1 shows the thermomechanical measurement system utilized here.[6] The sample was connected with quartz rods, which were used as an adiabatic material, and suspended vertically inside the thermocontrolled copper chamber under a constant weight. The applied load was monitored, during the measurement, by a load cell, from which the tensile stress σ was calculated by using the cross-sectional area of the sample. The strain was calculated as $\epsilon = \Delta L/L$, where ΔL is a change in sample length L and is detected by using a linear variable differential transformer (LVDT). Temperature T of the sample was measured by a chromel–alumel thermocouple positioned near the center of the sample. The ΔL versus T curve was recorded on an X–Y recorder. Thus obtained curves were digitalized and analyzed by using a microcomputer.

X-ray Diffraction Measurement under Tension. The X-ray diffraction measurement under a constant tensile stress was carried out with a sample elongation device shown in Figure 2. Ni-filtered Cu Kα radiation ($\lambda = 0.1542$ nm) was used as an X-ray source. The diffracted beams were detected with a proportional photon counter. The uniaxially oriented sample rod was set horizontally in the cell with one end fixed on a load cell and another end connected to a static weight. The X-ray profile of the (00l) reflections was measured by a θ–2θ scanning method at a constant temperature.

Samples. The samples were VDF–TrFE copolymers with VDF contents of 0–73%, which were supplied by Daikin Kogyo Co., Ltd. Japan. Uniaxially oriented samples were prepared by elongating the solution-cast film about 5 times the original length at room temperature.

Results and Discussion

Macroscopic Dimensional Change and Phase Transition. Figure 3 shows the temperature dependence of the sample length measured for the as-drawn VDF 65% copolymer sample. In the first run, the sample contracted remarkably as the temperature rose and did not regain the original length even after cooling down to the room temperature. After several cycles of heating and cooling, the curve became an almost completely closed loop. All the data shown in the following sections are the curves thus obtained. In Figure 4 is compared the thermal contraction curve with the temperature dependence of X-ray diffraction, infrared, and DSC data for VDF 65% sample.[3] The crystalline region of the annealed VDF 65% sample is composed of the mixture of the regular low-temperature phase and the irregular cooled phase.[3,7] These phases exhibit a different transitional behavior from each other as stated in ref 3. The double peaks around 80 °C (heating) and 60 °C (cooling) in the DSC curve may correspond to these transitions. In this transitional region, the X-ray diffraction and infrared absorption intensities change drastically. The thermal contraction curve also shows a large change in the vicinity of the transition region.

Similar correspondence between the structural data and the thermal contraction behavior is also seen for the case of VDF 73% copolymer. Figure 5a shows the temperature dependence of the infrared absorbances for the trans and gauche bands in comparison with the thermal contraction curve. In Figure 5b are shown the DSC curves. In the heating process the sample length begins to contract at 90–110 °C, where the infrared bands begin to change their intensity and the DSC curve shows the subpeak. Near 120 °C the sample begins to melt, as seen in the DSC curve and also in the decrease in the infrared absorption of both the trans and gauche crystalline bands, where the sample length begins to contract with much steeper rate than in the phase-transition region. Upon cooling the sample at this stage, it elongates back to the value before the beginning of melting. In the vicinity of the transition point (about 70 °C), where the DSC subpeak appears and the trans–gauche exchange is observed for the infrared spectral data, a remarkably large thermal expansion occurs and the sample length becomes almost equal to the original value, although some elongation is detected because of the loading of a weight.

0024-9297/88/2221-2463$01.50/0

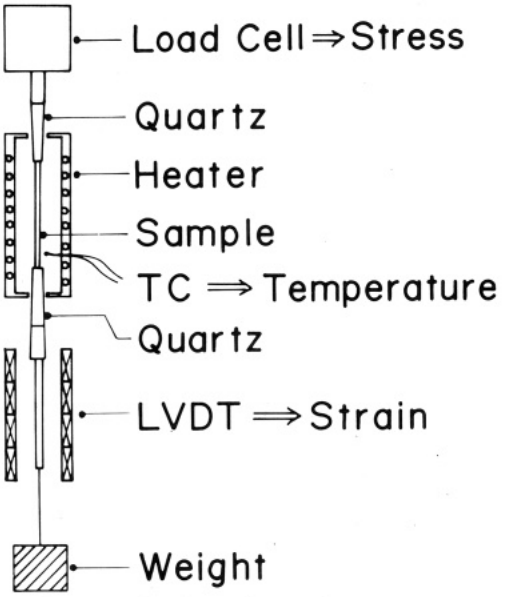

Figure 1. Apparatus for thermal expansion measurements under tensile stress.

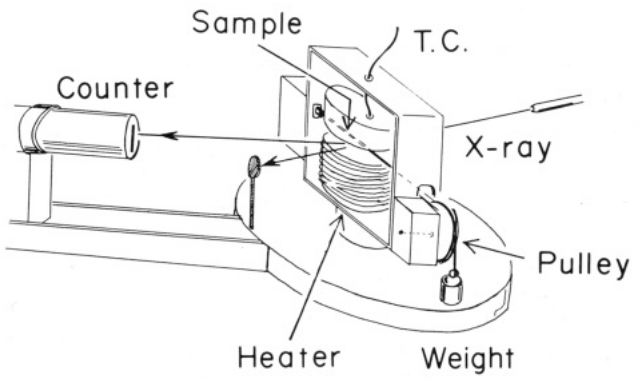

Figure 2. X-ray measuring system with a stress loading instrument and a thermocontrolled cell.

Figure 6 shows the thermal contraction curves measured for the oriented VDF 0–73% copolymer samples. As the VDF content increases, the dimensional change becomes clearer in the narrower temperature region. At the same time, the thermal hysteresis also becomes more appreciable. These observations are completely parallel with the infrared and X-ray diffraction data reported in ref 3. Based on all the experimental data presented in Figures 4–6, we may say that the macroscopic thermal contraction behavior reflects directly the phase transition in the crystalline region for all the members of the VDF–TrFE copolymers.

Let us consider a simple series model of the crystalline and amorphous phases. The macroscopic dimensional change ΔL may be expressed as follows:

$$\Delta L = \Delta L_c + \Delta L_a \quad (1)$$

where L_c and L_a are the lengths of the crystalline and amorphous phases along the draw direction, respectively. Then, the strain is given as

$$\Delta L/L = (\Delta L_c/L_c)(L_c/L) + (\Delta L_a/L_a)(L_a/L) \quad (2)$$

that is,

$$\epsilon = \epsilon_c x + \epsilon_a(1 - x) \quad (3)$$

where x is a degree of crystallinity. In the phase-transition region ($\Delta T \sim 45$ °C), the crystalline phase contracts by about 9.8% along the c-axis.[1-3] In this temperature region, the macroscopically observed value ϵ is about 3.3% as seen in Figures 3 and 4, for example. Assuming x is about 0.5, the amorphous phase is estimated to change by about

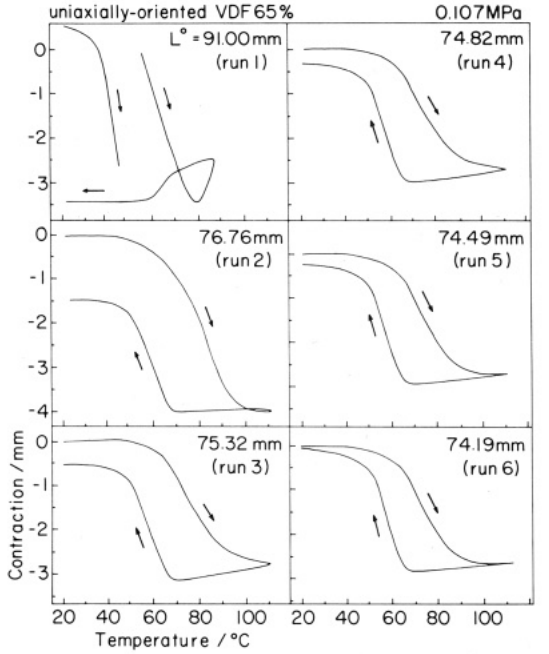

Figure 3. Thermal contraction curves along the draw axis of the uniaxially oriented VDF 65% copolymer under tensile stress of 0.107 MPa. It should be noticed that the curve is almost completely closed after several runnings. The curve of run 1 in the region of 20–50 °C is intentionally shifted 4 mm along the vertical axis because of too large a contraction of the sample length: the extension of this curve joins with another part at ca. 55 °C.

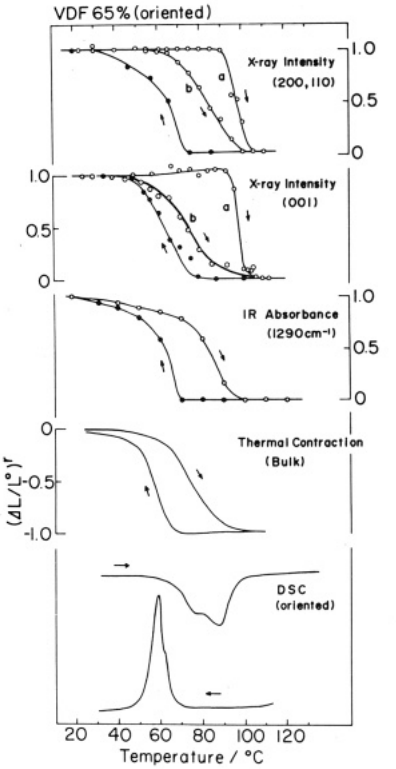

Figure 4. Comparison of the temperature dependences of X-ray intensity, infrared absorbance of the trans band (1290 cm^{-1}), dimensional change, and DSC curve for the uniaxially oriented VDF 65% sample. The (a) and (b) in the X-ray (200, 110) and (001) reflection intensity curves represent respectively the cases of the sample with the low-temperature phase and the sample with a mixture of the cooled phase and the low-temperature phase. The usually obtained sample corresponds to the latter case, as used in the present thermal contraction measurement.

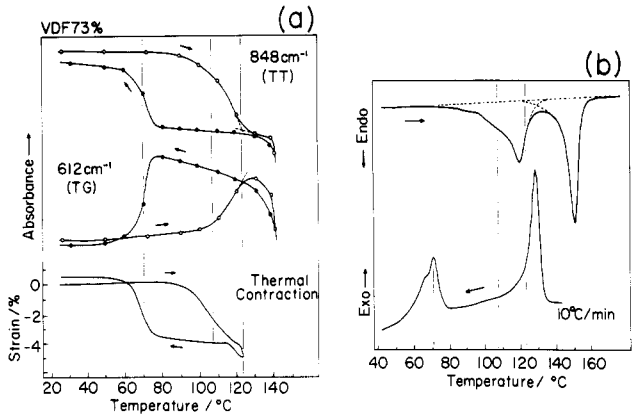

Figure 5. (a) Thermal contraction curve in comparison with the temperature dependence of the infrared absorbances of the trans and gauche bands and (b) the DSC curves measured for the uniaxially oriented VDF 73% copolymer sample.

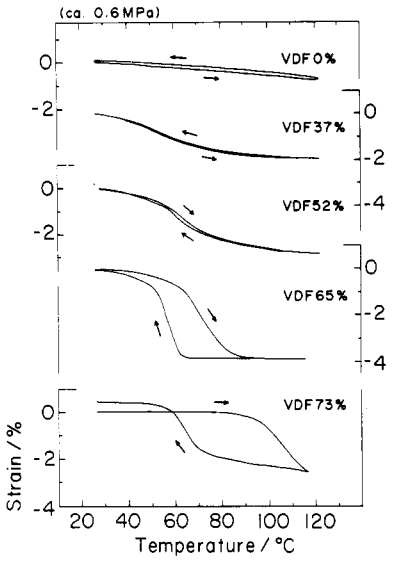

Figure 6. Thermal contraction curves of the oriented VDF 0–73% copolymers under stress of about 0.6 MPa.

−3.2%. This negative value corresponds to the thermal "expansion" coefficient of about 7×10^{-4} K^{-1}, which is a reasonable value, comparable to those reported for the amorphous phases in general polymers. That is to say, in the temperature region of the structural phase transition, the crystalline phase contracts along the *c*-axis from the trans to gauche forms, whereas the amorphous phase experiences thermal expansion. The dimensional changes are cancelled in part by each other, resulting in a relatively small value of the macroscopically observed thermal contraction compared with that expected for the crystalline region.

In this way, an intimate relationship is seen between the macroscopically observed thermal contraction and the crystalline phase transition. Is there any possibility of assigning the macroscopic dimensional change to another phenomenon, e.g., the so-called rubber elastic effect? For flexible polymers such as polyethylene,[8,9] nylon 6,[10] etc., there is observed a remarkably large thermal contraction for oriented samples, even larger than the contraction of the crystalline *c*-axis. Choy et al.[8] ascribed this phenomenon to the rubber elastic effect of the amorphous regions with the apparent cross-linkages due to the crystalline bridges. But such behavior is characteristic of the oriented sample drawn to relatively low elongation and is not observed for the highly oriented case, where the thermal expansivity approaches the crystalline value. Furthermore,

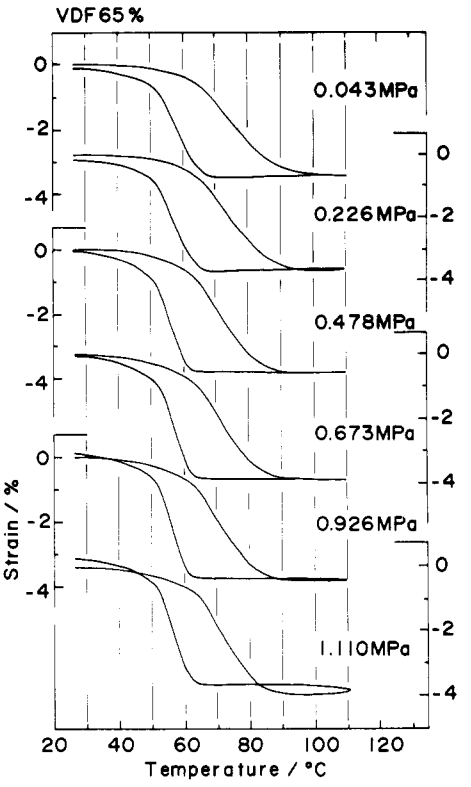

Figure 7. Stress dependence of thermal contraction curve of the VDF 65% copolymer.

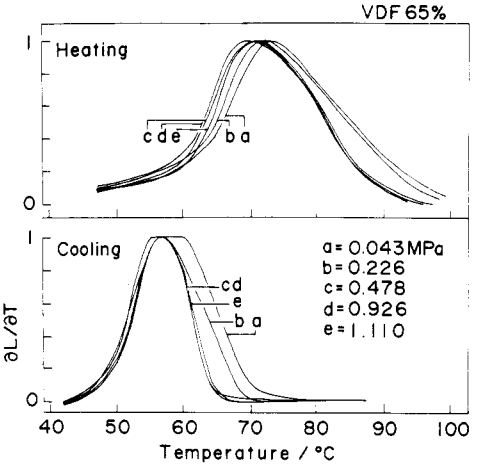

Figure 8. Differentiated curves of Figure 7 with respect to temperature.

the rubber elasticity should be much more emphasized at the higher temperature, i.e., the sample is expected to contract increasingly as the temperature increases. Such a phenomenon, however, is not observed for the present case of the copolymers: the sample length is almost constant at high temperature above the phase transition point. In addition, as shown in Figures 4–6, the thermal contraction behavior corresponds quite well to the crystalline phase transition. Therefore, under these circumstances, we may say that a rubber effect may not contribute so significantly to the macroscopic thermal contraction of the copolymer.

Effect of Tensile Stress on the Thermal Contraction Curves. Figure 7 shows the stress dependence of the thermal contraction curves for the uniaxially oriented and annealed VDF 65% copolymer sample. In Figure 8 are shown the differentiated curves of Figure 7 with respect to temperature. The maximal point of the differentiated curve, which corresponds to the temperature region of

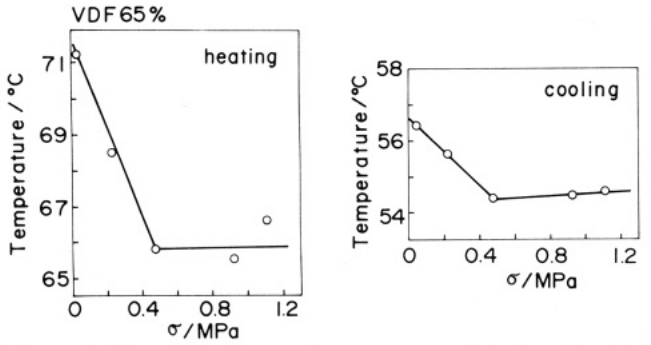

Figure 9. Transition temperature versus applied stress for the VDF 65% copolymer.

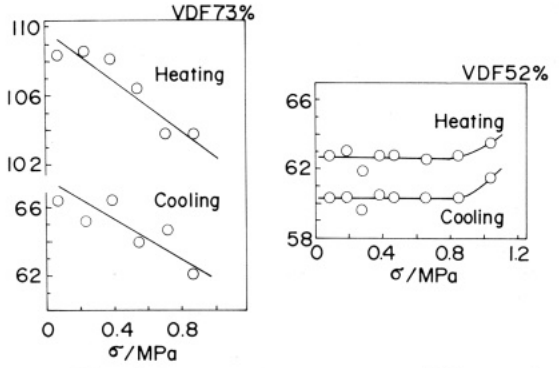

Figure 10. Transition temperature versus applied stress for the VDF 52 and 73% copolymers.

steepest change in the sample dimension, shifts to the lower temperature side as the applied tensile stress is increased. In Figure 9, the temperatures of these maximal points are plotted against the tensile stress for the heating and cooling processes. In the low-stress region, the curve is almost linear; the rate of shift is evaluated as ca. −12 °C/MPa for the heating process and ca. −5 °C/MPa for the cooling process. Figure 10 shows the similar plots for VDF 52 and 73% samples. For the VDF 73% sample, the slope is about −6 °C/MPa. In the VDF 52% sample, such a tendency is not observed so clearly, but in the large tensile stress region, the transition temperature is found rather to shift toward the higher temperature side. This phenomenon is observed also for the VDF 65% sample as seen in a large stress region of Figure 9.

As discussed in the previous section, the macroscopic thermal contraction reflects the dimensional change in the ferroelectric phase transition of the crystalline region. Therefore, it may be reasonable to assume that the transition temperature shift originates from the stress effect on the crystalline phase transition. Before discussing such an effect in the crystalline phase, we must take into account some influence by the amorphous phase. The externally applied stress might induce the crystallization of some parts in the amorphous phase. The thermal expansion of the amorphous phase might be also affected by the tensile stress. Thus, as a trial, we calculated the macroscopic thermal contraction curves under the assumptions that (i) the series model of the crystalline and amorphous phase is employed, (ii) the dimensional behavior of the crystalline region is not affected by the external stress, and (iii) the thermal expansivity of the amorphous phase is affected by the stress. We assume the thermal strain of the amorphous phase is expressed as follows:

$$\epsilon_a = \alpha T + \beta T^2 + \gamma \tag{4}$$

Where T is a temperature and α, β, and γ are the constants. Substitution of eq 4 into eq 3 leads us to calculate the temperature dependence of $\Delta L/L$, just when the curve for ϵ_c is assumed to be given by

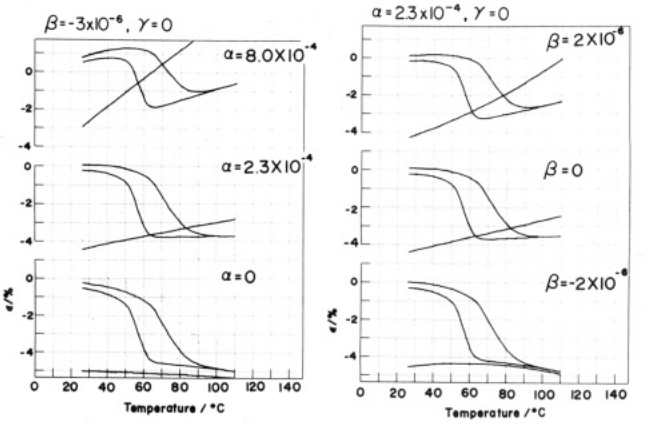

Figure 11. Calculated thermal contraction curves for the various values of the parameters α and β in eq 4 in the text. The assumed thermal expansion curves of the amorphous part are also included here.

$$\epsilon_c = -0.098(1 - p_t) \tag{5}$$

where the c-axis dimension in the trans form is taken as a basis for ϵ_c and p_t is a trans fraction given by the X-ray intensity or infrared data.[3] The crystallinity is assumed to be 0.5. In Figure 11, are shown some calculated sets of the curves for the various values of the parameters α and β. As seen here, a macroscopically observed transition point shifts only by 10^{-3} °C even when the parameters are varied, exceeding the generally accepted values. That is to say, an effect of the external stress on the thermal behavior of the amorphous phase may be negligibly small.

As another effect we consider the shift of the crystalline phase transition point. The effect of an external force on the phase transition point is now discussed in terms of a thermodynamical free energy. For the change in the external field, the free energy change per unit volume of crystal $d\bar{G}$ is given by

$$d\bar{G} = -\bar{S}\, dT - \epsilon_{ij}\, d\sigma_{ij} - P_m\, dE_m \tag{6}$$

where $\bar{S}$ is an entropy per unit volume, ϵ is a strain, σ is a stress, P is an electric polarization, and E is an electric field strength.

We consider first the case of hydrostatic pressure p. The stress is expressed as follows:

$$\sigma_{ij} = -p\delta_{ij} \tag{7}$$

where δ_{ij} is Kronecker's delta. From eq 6 and 7, $d\bar{G}$ is written as

$$d\bar{G} = -\bar{S}\, dT + \epsilon_{ij}\delta_{ij}\, dp \tag{8}$$

The equilibrium condition of the two phases α and β is given by

$$d\bar{G}_\alpha = d\bar{G}_\beta \tag{9}$$

Thus, from eq 8 and 9, we obtain

$$dT/dp = [(\epsilon_{11} + \epsilon_{22} + \epsilon_{33})_\beta - (\epsilon_{11} + \epsilon_{22} + \epsilon_{33})_\alpha]/(\bar{S}_\beta - \bar{S}_\alpha) \tag{10}$$

$(\epsilon_{11} + \epsilon_{22} + \epsilon_{33})_\beta - (\epsilon_{11} + \epsilon_{22} + \epsilon_{33})_\alpha$ is given by $\Delta V/V^0$, where ΔV is a volume difference between the α and β phases. Putting V^0 as unity, we obtain finally

$$dT/dp = \Delta V/\Delta\bar{S} \qquad (\Delta = \beta - \alpha) \tag{11}$$

Since the changes in both volume and entropy in the

ferroelectric phase transition of the copolymers are positive in the heating process, $dT/dp > 0$; i.e., the transition point is expected, from eq 11, to rise as the static pressure increases. Koizumi et al.[11] measured the hydrostatic pressure dependence of the linear expansion for the unoriented bulk VDF 53% copolymer: the transition point is observed to shift to the higher temperature with an increase in the hydrostatic pressure.

Next, the effect of tensile stress σ_3 ($=\sigma_{33}$) along the chain axis will be discussed. Under constant electric field strength, the free energy change of eq 6 is expressed as

$$d\bar{G} = -\bar{S}\,dT - \epsilon_3\,d\sigma_3 - \epsilon_1\,d\sigma_1 - \epsilon_2\,d\sigma_2 \qquad (12)$$

In the actual sample the crystallite is connected to the amorphous phase and therefore the sides of the crystallite are not necessarily free of stress but the stress tensor components σ_1 and σ_2 also work on the crystallite as inner stress, as seen in eq 12. The boundary conditions are given as follows:[12] (i) the stress of the amorphous phase σ_{ai} and that of the crystallite σ_i (i = 1 and 2) are balanced to each other, i.e., $\sigma_i = -\sigma_{ai}$ (the crystallinity 0.5 assumed) and (ii) the strains of the amorphous (ϵ_{ai}) and crystalline (ϵ_i) phases at the boundary are equal to each other, i.e., $\epsilon_i = \epsilon_{ai}$. Besides, in a mechanical series model, $\sigma_3 = \sigma_{a3}$.

As is well-known,

$$\epsilon_i = \sum_j s_{ij}\sigma_j \quad \text{and} \quad \epsilon_{ai} = \sum_j s_{aij}\sigma_{aj} \qquad (i = 1, 2;\ j = 1\text{–}3) \qquad (13)$$

where s is the compliance tensor component. Using the definition of the Poisson's ratio ($\nu_{ij} = -s_{ij}/s_{jj}$) and Young's modulus ($E_i = 1/s_{ii}$, $E_a = 1/s_{a11} = 1/s_{a22} = 1/s_{a33}$) and assuming that the compliance tensor components s_{ij} in the lateral direction of the crystal (s_{11}, s_{22}, s_{12}) are equal to those of the isotropic amorphous phase, the following equations are obtained:

$$\sigma_1 = \sigma_2 = (\nu E_a/E_3 - 0.5)\sigma_3 \qquad (14)$$

where we assumed that

$$\nu = \nu_{13} = \nu_{23}$$

and

$$\nu_{a13} = \nu_{a12} = \nu_{12} \doteq 0.5$$

By use of eq 14, the strains ϵ_1 and ϵ_2 are calculated from eq 13, and then the free energy change in eq 12 is expressed as

$$d\bar{G} = -\bar{S}\,dT - k\epsilon_3\,d\sigma_3 \qquad (15)$$

where

$$k = 1 - \frac{4\nu^2 - p^2}{4[(1+\nu)p - 2\nu^2]} \qquad (16)$$

and $p = E_3/E_a$. From the equilibrium condition of eq 9, we obtain

$$\begin{aligned} \Delta\bar{S}\,dT &= -(k_\beta\epsilon_{3\beta} - k_\alpha\epsilon_{3\alpha})\,d\sigma_3 \\ &= [-k_\beta(\Delta l/l^0) - (k_\beta - k_\alpha)\epsilon_{3\alpha}]\,d\sigma_3 \\ &= -k_\beta(\Delta l/l^0)\,d\sigma_3 \end{aligned} \qquad (17)$$

where the second term due to the elastic strain $\epsilon_{3\alpha}$ is neglected because the change in the fiber period at transition ($\Delta l/l^0$) is much larger than such an elastic strain. Thus we obtain

$$dT/d\sigma_3 = -k_\beta(\Delta l/l^0)/\Delta\bar{S} \qquad (18)$$

In the cooling process, for example, the repeating period along the c-axis is expanded by 9.8% ($=\Delta l/l^0$) and the entropy decreases by $\Delta\bar{S} = -12.4 \times 10^4$ J/Km^3 (x = 0.5 assumed).[13] In the vicinity of the transition point the Young's modulus decreases by a factor of 4–5 even for the unoriented bulk sample[14,15] because of the large conformational change occurring in the crystalline phase. This factor of decrease in modulus may be much higher for the crystalline modulus E_3 along the chain axis. Then E_3 at the transition point is assumed here ca. 15 GPa, referring to the crystallite moduli of PVDF forms I and II[16] and the effective cross-sectional area of the chain. The modulus E_a is assumed as 2 GPa. The Poisson's ratio ν of the crystalline phase is far larger than the usual value of ca. 0.5. In the present case ν is estimated as ca. 4–5 by the X-ray diffraction measurements, which is close to the values for PVDF[17] and PE.[18] This unusually large ν may come from (i) the inner stress effect (σ_1) due to the boundary condition[18] and (ii) the thermally induced flexural motion of the chain;[19] the tensile stress decreases the thermal amplitude of the chain, resulting in the additional contraction of the lateral spacing of the cell. Then Poisson's ratio ν is tentatively assumed here as ca. 4.5. By use of these parameters, $dT/d\sigma_3$ is calculated as –5.7 °C/MPa from eq 18. This value may be consistent with the experimentally evaluated value of about –5 °C/MPa (Figure 9).

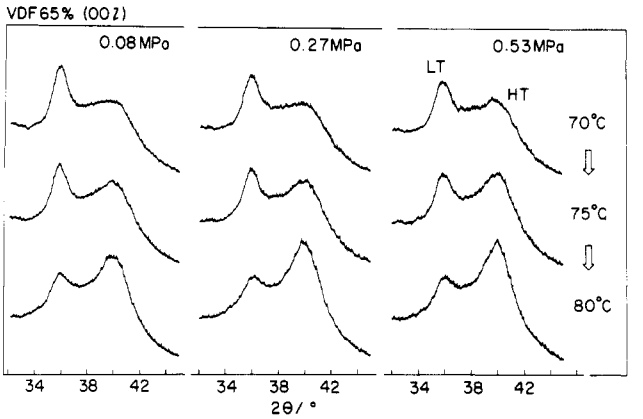

Figure 12. Temperature dependence of the X-ray diffraction profile of the VDF 65% (001) reflection.

In order to confirm the above consideration that the macroscopically observed stress dependence of the transition temperature may originate from the effect in the crystalline phase, we tried to measure the temperature dependence of the X-ray diffraction intensity under the application of the external stress. In Figure 12 is shown the temperature dependence of the X-ray diffraction profile for the VDF 65% (00l) reflections. By comparing the X-ray reflection profiles under varied tensile stress at 75 °C, for example, we notice that as the applied stress is increased, the intensity of the high-temperature (HT) phase ($2\theta \sim 41$ deg) increases relatively to that of the low-temperature (LT) phase ($2\theta \sim 36$ deg). This suggests that the phase transition under the high stress occurs at the lower temperature side than that of the low stress. Figure 13 shows a temperature dependence of the integrated X-ray intensity of the trans phase ($2\theta \sim 36°$). As the stress increases, the curve appears to shift toward the lower temperature side. The rate of shift $dT/d\sigma_3$ is estimated as about –7 °C/MPa, which agrees well with the thermodynamically estimated value –6 °C/MPa and the macroscopically observed value –5 °C/MPa. In Figure 14 are shown some examples of the macroscopic thermal contraction curves calculated by taking into account the confirmed transition point shift of the crystalline phase as well as the thermal expansion of the amorphous phase.

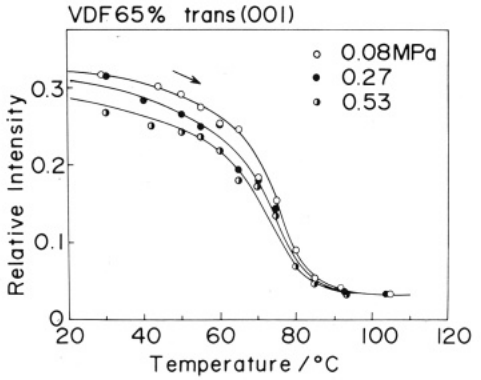

Figure 13. Temperature dependence of the integrated intensity of the (001) X-ray reflection for the VDF 65% copolymer trans phase.

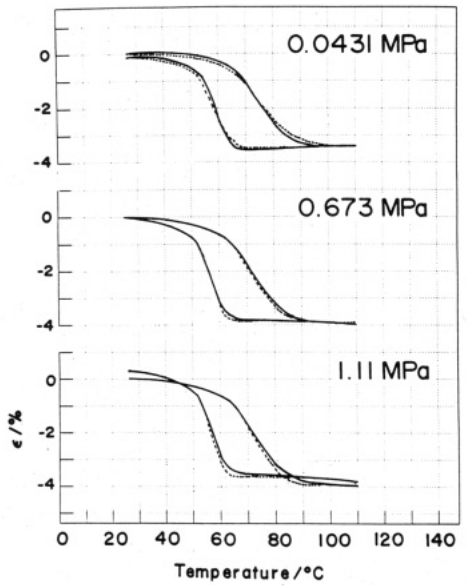

Figure 14. Calculated thermal contraction curves for VDF 65% copolymer sample. Broken line represents the observed curve.

In this way we have found that the external tensile stress applied along the draw axis causes the low temperature shift of the phase transition point. This phenomenon is contrary to the case of the hydrostatic pressure described above. From the thermodynamical point of view, the transition temperature is considered as a cross point of the $\bar{G}$ versus T curves of the two phases where $\bar{G}$ and T denote the free energy and temperature, respectively. Under the application of the external force field, the free energies of both phases may be increased or decreased than the initial values, resulting in a shift of the transition point. Figure 15 illustrates the $\bar{G}$ versus T curves for the α (low-temperature) and β (high-temperature) phases, where $\bar{G}_\alpha$ is shifted relatively to $\bar{G}_\beta$ so as to simplify the situation. The relative free energy of the α phase is increased by tensile force and decreased by hydrostatic pressure. As a result, the cross point of $\bar{G}_\alpha$ and $\bar{G}_\beta$ or the transition temperature increases as the higher hydrostatic pressure is applied, while it decreases with an increment of the tensile stress. Such a free energy variation with tensile stress may be originated from the k value in eq 18 or the unique Poisson's ratio of the polymer crystal, as described above.

Phase Transition in Large Tensile Stress Region. As discussed above, the phase-transition behavior under small tensile stress may be described by the so-called Clausius–Clapeyron equation (eq 18). Under larger tensile stress, however, the transition point shifts rather to the higher temperature side (see Figures 9 and 10) for the cases

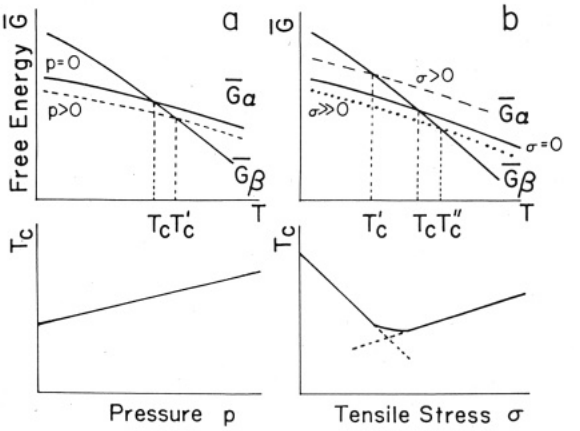

Figure 15. Free energy as a function of temperature for the two phases of α (trans) and β (gauche): (a) a case of hydrostatic pressure p and (b) a case of tensile stress σ. For the VDF 52 and 65% samples, which include the cooled phase with some fractions, the high stress σ induces the phase transition of the irregular cooled phase to the regular low-temperature phase and as a result the free energy is decreased (the dotted curve in this figure) and the transition point apparently shifts toward the higher temperature side. The lower figures show the predicted stress dependence of the transition point T_c for these cases.

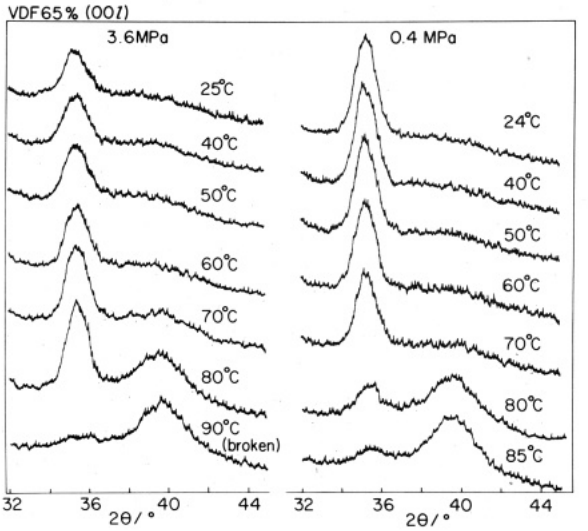

Figure 16. Temperature dependence of the X-ray meridional reflection profile measured for the VDF 65% copolymer under tensile stress.

of VDF52 and 65% samples.

In Figure 16 is shown the temperature dependence of the X-ray (00l) reflection profile under a large tensile stress for the oriented VDF 65% sample compared with that taken under small tensile stress. Under the high stress, the reflection intensity of the trans phase increases as the temperature rises and thus the transition point shifts apparently to the higher temperature side. At 90 °C, the sample was broken before the complete transformation to the high-temperature phase. The application of enough high stress was reported to transfer the cooled phase into the regular low-temperature phase at room temperature, the transition point of which is much higher than that of the cooled phase.[2,3,7] That is to say, the large tensile stress is considered to induce the disorder-to-order transition in the cooled phase. The increasing intensity of the trans reflection at higher temperature suggests that such a transition is more enhanced at higher temperature than at room temperature.

In the representation of free energy shown in Figure 15b, we may say that for VDF 52 and 65% samples containing

some amounts of the cooled phase, the high tensile stress lowers the free energy of this trans phase compared to that under free tension because of the occurrence of the phase transition to the thermodynamically more stable trans form. The crossing of the transition point shifts to the higher temperature side. The T_c, plotted against tensile stress σ, is expected to change as illustrated in the lower half-side of Figure 15b. This is consistent with the experimental result shown in Figures 9 and 10.

Conclusion

In the present paper we have discussed the effect of tensile stress on the ferroelectric phase transition of the VDF–TrFE copolymer system based on the measurement of the thermally induced dimensional change along the chain direction.

The tensile stress lowers the crystalline transition point at a rate of ca. $-4 \sim -7$ °C/MPa. The X-ray diffraction measurement under tension supported this conclusion. An application of the modified Clausius–Clapeyron equation was found to be useful for interpretation of the phenomenon. In a high tensile stress region, on the other hand, the structurally disordered cooled phase is forced to transform to the regular low-temperature phase, resulting in the rather high-temperature shift of the transition point for VDF 52 and 65% samples.

What happens when the tensile force is applied in the direction perpendicular to the chain axis? The experimental results will be reported in the next paper of this series.

Acknowledgment. We are grateful to Daikin Kogyo Company, Ltd., Japan for supplying the samples of VDF–TrFE copolymers as well as for use of their X-ray diffractometer. This work was supported in part by a Grant-in-Aid on Special Project Research for "Organic Thin Films for Information Conversion" from the Ministry of Education, Science and Culture, Japan.

Registry No. (VDF)(TrFE) (copolymer), 28960-88-5.

References and Notes

(1) Tashiro, K.; Takano, K.; Kobayashi, M.; Chatani, Y.; Tadokoro, H. *Polymer* **1981**, *22*, 1312.
(2) Tashiro, K.; Takano, K.; Kobayashi, M.; Chatani, Y.; Tadokoro, H. *Polymer* **1984**, *25*, 195.
(3) Tashiro, K.; Takano, K.; Kobayashi, M.; Chatani, Y.; Tadokoro, H. *Ferroelectrics* **1984**, *57*, 297.
(4) Lovinger, A. J.; Davis, G. T.; Furukawa, T.; Broadhurst, M. G. *Macromolecules* **1982**, *15*, 323.
(5) Lovinger, A. J.; Davis, G. T.; Furukawa, T.; Broadhurst, M. G. *Polymer* **1983**, *24*, 1225, 1233.
(6) Ii, T.; Tashiro, K.; Kobayashi, M. *Macromolecules* **1986**, *19*, 1809.
(7) Tashiro, K.; Kobayashi, M. *Polymer* **1986**, *27*, 667.
(8) Choy, C. L.; Chen, F. C.; Young, K. *J. Polym. Sci., Polym. Phys. Ed.* **1981**, *19*, 335.
(9) Orchard, G. A. J.; Davis, G. R.; Ward, I. M. *Polymer* **1984**, *25*, 1203.
(10) Choy, C. L.; Leung, W. P.; Ong, E. L. *Polymer* **1985**, *26*, 884.
(11) Koizumi, N.; Murata, Y.; Oka, Y. *Jpn. J. Appl. Phys.* **1984**, *23*, L324.
(12) Sawatari, C.; Matsuo, M. *Macromolecules* **1986**, *19*, 2726.
(13) Koizumi, N.; Haikawa, N.; Habuka, H. *Ferroelectrics* **1984**, *57*, 99.
(14) Murata, Y.; Koizumi, N. *Rep. Progr. Polym. Phys. Jpn.* **1987**, *30*, 363.
(15) Tashiro, K.; Nishimura, S.; Kobayashi, M. *Rep. Progr. Polym. Phys. Jpn.* **1987**, *30*, 355.
(16) Tashiro, K.; Kobayashi, K.; Tadokoro, H. *Macromolecules* **1977**, *10*, 731.
(17) Tasaka, S.; Miyata, S. *Ferroelectrics* **1981**, *32*, 17.
(18) Miyasaka, K.; Makishima, K. *Kobunshi Kagaku* **1966**, *23*, 785.
(19) Ii, T.; Tashiro, K.; Kobayashi, M.; Tadokoro, H. *Proc. Am. Chem. Soc., Div. Polym. Mater. Sci. Eng.* **1986**, *55*, 826.

Effect of Crystallization Condition on the Ferroelectric Phase Transition in Vinylidene Fluoride/Trifluoroethylene (VF_2/F_3E) Copolymers

Hajime Tanaka,* Hideyuki Yukawa,† and Toshio Nishi

Department of Applied Physics, Faculty of Engineering, The University of Tokyo, Bunkyo-ku, Tokyo 113, Japan. *Received November 10, 1987*

ABSTRACT: We report the effects of crystallization temperature on thermal properties of the ferroelectric transitions of random copolymers of vinylidene fluoride (VF_2) and trifluoroethylene (F_3E). We find that the Curie point decreases as the crystallization temperature increases. In the copolymer containing 65 mol % VF_2, two peaks corresponding to the Curie transitions are observed only when the copolymer is crystallized in a paraelectric phase. The results clearly indicate that the crystalline structure of the ferroelectric phase strongly depends on the crystallization temperature, especially on whether a copolymer is crystallized above or below the Curie point. This can be understood by the imperfection of the solid–solid transformation of the crystalline structure from the paraelectric to the ferroelectric phase. A phase diagram containing two kinds of ferroelectric phases has been proposed.

Introduction

Since the discovery of the ferroelectric phase transition in random copolymers of vinylidene fluoride (VF_2) and trifluoroethylene (F_3E),[1–7] the ferroelectric transition has been extensively studied by many researchers.[1–13] The crystalline structures have been studied in detail by X-ray diffraction measurements, and the structural change accompanied by the ferroelectric phase transition has been made clear.[8–13] The transition from the ordered ferroelectric phase to the disordered paraelectric phase is ascribed to the structural and conformational change of molecular chains inside the crystal. Spectroscopic studies using Raman scattering and infrared absorption also support the conformational change by the transition.[11–13]

†Current address: Mazda Motor Corporation, Hiroshima City, Hiroshima, Japan.

0024-9297/88/2221-2469$01.50/0